

AperTO - Archivio Istituzionale Open Access dell'Università di Torino

## Micro porous carbon spheres from cyclodextrin nanosponges

### This is the author's manuscript

*Original Citation:*

*Availability:*

This version is available <http://hdl.handle.net/2318/1591989> since 2019-02-11T14:30:02Z

*Published version:*

DOI:10.1016/j.micromeso.2016.08.012

*Terms of use:*

Open Access

Anyone can freely access the full text of works made available as "Open Access". Works made available under a Creative Commons license can be used according to the terms and conditions of said license. Use of all other works requires consent of the right holder (author or publisher) if not exempted from copyright protection by the applicable law.

(Article begins on next page)



## UNIVERSITÀ DEGLI STUDI DI TORINO

This Accepted Author Manuscript (AAM) is copyrighted and published by Elsevier. It is posted here by agreement between Elsevier and the University of Turin. Changes resulting from the publishing process - such as editing, corrections, structural formatting, and other quality control mechanisms - may not be reflected in this version of the text. The definitive version of the text was subsequently published in *Microporous and Mesoporous Materials* 235 (2016) 178-184.

You may download, copy and otherwise use the AAM for non-commercial purposes provided that your license is limited by the following restrictions:

- (1) You may use this AAM for non-commercial purposes only under the terms of the CC-BY-NC-ND license.
- (2) The integrity of the work and identification of the author, copyright owner, and publisher must be preserved in any copy.
- (3) You must attribute this AAM in the following format: Creative Commons BY-NC-ND license (<http://creativecommons.org/licenses/by-nc-nd/4.0/deed.en>), <http://dx.doi.org/10.1016/j.molcata.2012.03.019>]

# Micro Porous Carbon Spheres from Cyclodextrin Nanosponges

Marco Zanetti<sup>1,2,\*</sup>, Anastasia Anceschi<sup>1</sup>, Giuliana Magnacca<sup>1</sup>, Giulia Spezzati<sup>3</sup>, Fabrizio Caldera<sup>1</sup>, Giovanni Paolo Rosi<sup>4</sup>, Francesco Trotta<sup>1</sup>

<sup>1</sup> University of Turin, Department of Chemistry, NIS Centre, INSTM, Via P. Giuria 7, 10125 Torino, Italy

<sup>2</sup> University of Turin, ICxT Centre, Lungo Dora Siena, 100, 10153 Torino, Italy

<sup>3</sup> Inorganic Materials Chemistry, Eindhoven University of Technology, P.O. Box 513, 5600MB, Eindhoven, The Netherlands

<sup>4</sup> Roquette Italia, Via Serravalle 26, 15063 Cassano Spinola, Italy

## Abstract

A series of carbons were prepared by pyrolysis of hyper cross-linked cyclodextrins, also known as nanosponges (NS). Pore structure analysis showed that pores with a range size of 5-16 Å can be created from  $\beta$ -CD an NS cross-linked with pyromellitic dianhydride (PY). NS cross-linked with hexamethylene diisocyanate (HD) was ineffective to produce pores. SEM observation reveals a peculiar morphology of the PY-NS carbon, made of perfectly spherical hollow particles. TGA and FT-IR studies demonstrate that the PY-NS is the more efficient carbon precursor.

Keywords: carbon, microporous carbon, cyclodextrin, hyper cross-linked cyclodextrins, nanosponges, carbonisation, pyrolysis, hollow spheres.

## 1. Introduction

Porous activated carbon materials are promising products in the fields of catalysis, supercapacitors and solid adsorbent materials for CO<sub>2</sub>. They are also used in the adsorption and storage of the carbon dioxide and in the removal of pollutants such as arsenic from water. Many porous materials based on carbon are known with different structures and morphologies and high surface areas. These materials are very convenient since they are cheap and show high thermal stability and high electrical conductivity.

According to IUPAC recommendation, there are three kinds of carbon porous materials: 1)

\* Corresponding Author, [marco.zanetti@unito.it](mailto:marco.zanetti@unito.it) (Marco Zanetti)

microporous materials having pores of diameter size less than 2nm; 2) mesoporous materials having pores with diameter size in the range from 2 to 50 nm; 3) macroporous materials having pores with diameter size higher than 50nm. Such porous materials are generally produced by pyrolysis of biomasses such as mushrooms, corn, lignocellulose materials, fish scales and starch [1]. In view of the interest generated by these porous products, many synthetic methods have been studied and applied.

In literature [2] the following synthesis methods are described: 1) chemical and physical activation and their combination; 2) catalytic activation of carbonious precursors by means of metal salts or organometals, 3) carbonization of an aerogel polymer in drying super-critical conditions; 4) carbonization of polymer mixtures of pyrolizable and carbonizable polymers; 5) biomass pyrolysis. These synthesis techniques allow mesoporous materials to be obtained.

The microporous materials are obtained by means of templates or through biomass pyrolysis [2]. In [3] a porous carbon material from resin pyrolysis is described. Specifically a solution of a cationic surfactant, formaldehyde, resorcinol,  $\text{Na}_2\text{CO}_3$  and deionized water was prepared, stirred and heated until the Krafft temperature of surfactant has been reached. After heating for 24 hours at  $70^\circ\text{C}$  (atmospheric pressure), a brown polymer was obtained. After drying, the polymer was carbonized at  $800^\circ\text{C}$ . The BET specific surface area was about  $500\text{m}^2/\text{g}$  after thermal treatment. Another porous material was obtained by pyrolysis of polysiloxanes: polymethyl(phenyl)siloxane was crosslinked at  $250^\circ\text{C}$  for 4 hours in air . The collected powder was pyrolyzed at  $1250\text{-}1450^\circ\text{C}$  under vacuum. Subsequently, the pyrolyzed samples were leached by hydrofluoric acid (HF) solution (40 vol. %) at room temperature for 1 h under stirring and rinsed off with distilled water to remove residue HF. It was then dried at  $110^\circ\text{C}$ . The leaching treatment was repeated for 5 times to prepare porous carbonaceous materials until there was no distinct weight loss. The porous material obtained showed pore diameter in the range of 2-3.2 nm and BET specific surface area in the range of  $650\text{-}1150\text{ m}^2/\text{g}$  in the tested temperature range [4].

K.T. Cho et al [5] used as precursor polyacrylonitrile. This precursor was oxidized at a temperature of  $290^\circ\text{C}$  for one hour through heating at a rate of  $2^\circ\text{C}/\text{min}$ . After thermal treatment, the mass was ground and mixed to KOH. The mixture was heated to  $700\text{-}800^\circ\text{C}$  for 1 or 2 hours under argon flux. The porous carbon so obtained after washing with HCl and rinsing with deionized water was dried in stove under vacuum at  $120^\circ\text{C}$ . The porous material so obtained showed a pore size distribution between 0,5 and 5 nm with a surface area above  $3000\text{ m}^2/\text{g}$ . The pore size distribution was between 5 and 50 A: this material resulted to be both microporous and mesoporous.

Many porous carbon materials deriving from biomasses showed high performances in many applications such as in the absorption of  $\text{CO}_2$  and in the removal of pollutants, for instance arsenic

in the water.

Some porous materials were obtained by the hydrochar, i.e. from the hydrothermal carbonisation of *Salix psammophila* [6]. The porous material so obtained is then activated under nitrogen at different temperatures for four hours at 4°C/min. After FTIR analysis the material resulted to have a condensate structure with BET specific surface area of 300m<sup>2</sup>/g and having micropores, mesopores and macropores.

Wang et al [7] used hydroxypropyl-β-cyclodextrin, which is a very expensive compound, to synthesize a mesoporous material, by preparing a composite with silica. Specifically hydroxypropyl-β-cyclodextrin is dissolved in water and then added with tetrahydroxysilane (TEOS). The mass is then left for three days with continuous removal of ethanol and then heated at 100°C for 12 hours. The final solid is then filtered and dried at 40°C. The material so obtained and consisting of HPCD/silica is then carbonised at 900°C in nitrogen. After the carbonisation the material is treated with hydrofluoric acid in order to remove silica. Following to the thermal initial treatment, BET specific surface areas between 500 and 1200 m<sup>2</sup>/g were obtained. The volume of the pores of the obtained material was between 0.11 and 1.22 cm<sup>3</sup>/g, the total volume of the micropores was between 0.022 and 0.239 cm<sup>3</sup>/g.

Cyclodextrins (CD) are nanometric biomaterials with a close relationship between molecular status and supramolecular properties [8,9]. They are a class of cyclic glucopyranose oligomers and are synthesised by enzymatic action on hydrolysed starch. The main common native CDs are α-, β- and γ-, which comprise six, seven and eight glucopyranose units, respectively. They have a characteristic toroidal shape, which forms a well-defined truncated cone-shaped lipophilic cavity able to include compounds whose geometry and polarity are compatible. They possess many desirable properties, such as a small molecular size (1.4–1.7nm) and reactive hydroxyl groups easily modified, being carriers for metal nanoparticle precursors, and low cost. In an earlier work we studied the carbonization pathway of α-CD and β-CDs derivatives, finding them capable to produce under pyrolysis condition valuable amounts of carbon [10]. More recently CDs have been taken as porogens and carbon precursors to yield nanoporous carbon materials: in [11,12] mesoporous carbons were prepared by a templating method using silica from tetramethyl orthosilicate as template to produce bimodal mesoporous carbons with 2.4 nm and ca. 24 nm diameter.

In this paper we describe our effort in producing a microporous carbon from hyper cross-linked CDs. Hyper cross-linked CDs are innovative cross-linked cyclodextrin polymers nanostructured within a three-dimensional network also known as Nanosponges (NS) [13]. This type of cyclodextrin polymer can form porous insoluble nanoparticles with a crystalline or amorphous structure and swelling properties. The polarity and dimension of the polymer mesh can be easily

tuned by varying the type of cross-linker and degree of cross-linking.

## 2. Experimental

### 2.1 Materials

-Cyclodextrin (  $\beta$ -CD) was provided by Roquette Italia SpA (Cassano Spinola, Italy). Pyromellitic dianhydride (PY), hexamethylene diisocyanate (HDI), dichloromethane, acetone, dimethyl sulfoxide (DMSO), triethyl amine (TEA) were purchased from Sigma–Aldrich (Munich, Germany) and used with no further purification.

The PY cross-linked NS (PY-NS) were prepared in 1:4 molar ratio of  $\beta$ -CD and PY. 11.35 g of anhydrous  $\beta$ -CD (10.00 mmol) and 17.45 g of PY (80.0 mmol) were dissolved in 100 mL of DMSO containing 2.7 mL TEA (19.4 mmol) and were allowed to react at room temperature for 3 h. Once the reaction was over, the solid obtained was ground in a mortar and Soxhlet extracted with acetone for 24 h. The HDI cross-linked NS (HD-NS) were prepared in 1:4 molar ratio of  $\beta$ -CD and HDI. 3.91g of anhydrous  $\beta$ -CD (3.44mmol) was added to 16 mL DMSO in round bottom flask to achieve complete dissolution by observing clear solution. Then, 4.64g of HDI (27.5mmol) was added as a cross-linking agent and the solution allowed reacting at 70°C for 4h. After the completion of the reaction, the solid block of cross-linked cyclodextrin was roughly ground in a mill and the unreacted reagents were completely removed by Soxhlet extraction with ethanol.

### 2.2 Carbon preparation

In a typical procedure 2g of precursor contained in a Coors combustion boat were inserted in a Lenton tubular furnace. The samples were then heated to 800°C with a heating ramp of 10°C/min under nitrogen flux (100 ml/min). The furnace was then cooled and the carbon was then maintained under nitrogen flux until the ambient temperature was reached. The carbon prepared from  $\beta$ -CD, PY-NS and HD-NS were named C-  $\beta$ -CD, C-PY-NS and C-HD-NS respectively.

### 2.3 Carbon Characterization

N<sub>2</sub> adsorption–desorption isotherms were measured at 77 K using a volumetric sorption analyzer (ASAP2020, Micromeritics). Prior to the adsorption measurements, the samples were degassed at 150 °C under vacuum (10  $\mu$ m Hg) for 12 h to remove the adsorbates and residual moisture. The specific surface area was estimated using the Langmuir equation, appropriate to describe the specific surface area of exclusively microporous systems, the total pore volume and size were

determined by means of DFT method applied to the adsorption branch of the isotherms (considering slit geometry and low regularization).

ATR infrared spectra were obtained with a Perkin-Elmer Spectrum 100 instrument equipped with a diamond single reflection ATR accessory. In the typical experiment, 32 scans were accumulated in the range of 4000-700  $\text{cm}^{-1}$  at  $4\text{cm}^{-1}$  resolution. The spectra were collected from the residues of TGA experiments stopped at various temperature.

Carbon morphology was observed by SEM (Leica Stereo-Scan 410) applying the accelerating voltage during scanning was 20 kV. Samples were mounted on metallic stubs with double-sided conductive tape and ion coated with gold by a sputter coater (Bal-tec SCD 050) for 60 s under vacuum at a current intensity of 60 mA.

TGA was performed on approx 10 mg samples in a TGA 2950 balance (TA Inc.) with alumina sample pan under a  $100\text{ cm}^3/\text{min}$  nitrogen flow (gas chromatography purity 99.999%) and with a  $10^\circ\text{C}/\text{min}$  heating ramp.

### 3. Results and discussion

The nitrogen adsorption isotherm curves of C- -CD(- -), C-PY-NS(- -) and C-HD-NS(- -) at 77 K are shown in Figure 1.

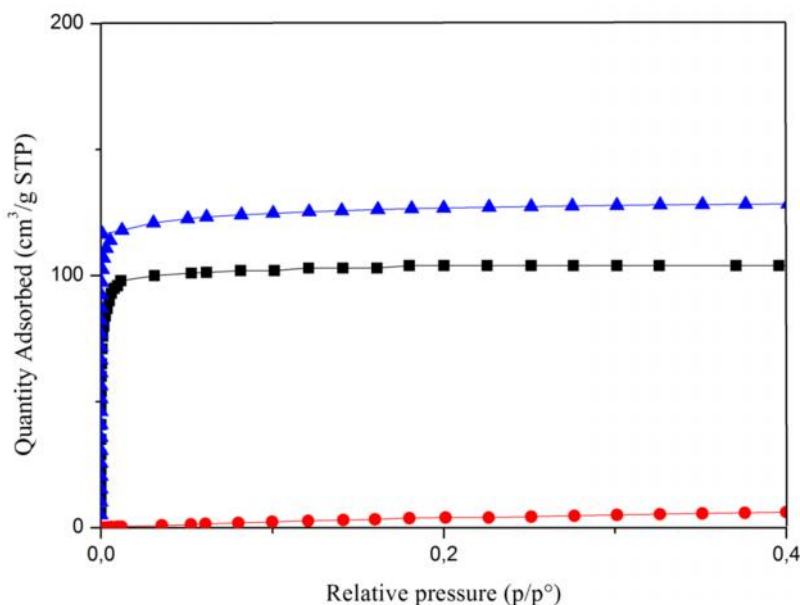


**Fig. 1:** Isotherm linear plot of C- -CD(- -), C-PY-NS(- -) and C- HD-NS(- -) at 77 K

The nitrogen adsorption isotherms of C- $\beta$ -CD, C-PY-NS show typical three steps with the increase in relative pressure. The first step is a steeply increasing region at low relative pressures less than 0.02, which stands for the adsorption or condensation in micropores. Then the adsorption amount remains almost constant, with no evidence of the presence of capillary condensation, indicating the absence of mesopores. Finally the adsorption amount increases abruptly at near the saturation pressure of nitrogen because of condensation phenomenon. This trend describes a type I isotherm according to the IUPAC classification, characteristic of microporous materials. All the physical characterization results of the analysed carbons based on the adsorption/desorption isotherms of nitrogen are listed in Table 1.

**Table 1:** Specific surface area, cumulative pore volume and pore width of different carbonized nanosponges

Sample	Surface Area $\text{m}^2/\text{g}$	Cumulative pore Volume $\text{cm}^3/\text{g}$	Pore width $\text{\AA}$
C- $\beta$ -CD	456	0.11	5-13
C-HD-NS	64	/	/
C-PY-NS	560	0.08	5-16

The C-HD-NS shows a specific surface area of  $64 \text{ m}^2/\text{g}$ , while the C- $\beta$ -CD, and C-PY-NS possess respectively  $456 \text{ m}^2/\text{g}$  and  $560 \text{ m}^2/\text{g}$ . Fig. 2 shows the pore size distribution curves for C- $\beta$ -CD and C-PY-NS obtained using DFT.

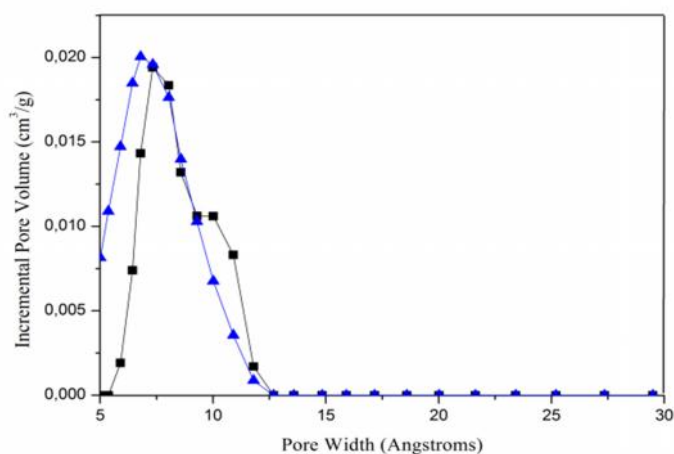


**Fig. 2:** Incremental pore volume vs. pore width of C- $\beta$ -CD(- -), C-PY-NS(- -).



In Fig. 2 the pore size distribution curve of the C-HD-NS is not reported because this carbon did not show a porous structure. The limit of the measurement is 5 Å, so all the curves starts from that value. However, the curves C- -CD have a peak in the range of 5-13 Å, corresponding to 0.11 cm<sup>3</sup>/g of total porosity, while the C-PY-NS shows a bimodal distribution in the range of 5-16 Å corresponding to 0.08 cm<sup>3</sup>/g of total porosity.

The pyrolysis of the three precursors led to the formation of different carbon morphology. Figure 3 shows SEM images of the -CD and of nanosponges before and after the carbonization.

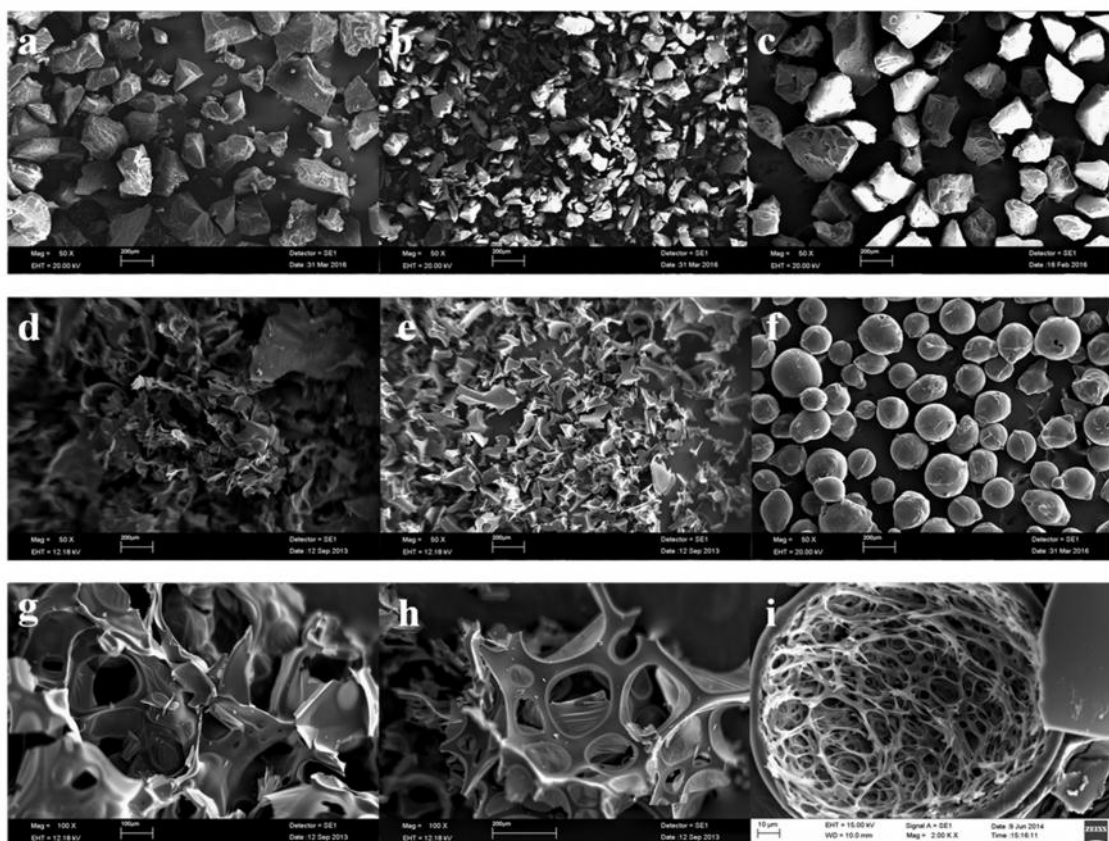


**Figure 3:** SEM imagines of -CD(a), nanosponges HD-NS (b), PY-NS (c) and carbons C- -CD(d,g), C- HD-NS(e,h) , C-PY-NS(f,i)

The -CD (Fig 3 a) shows a typical polyhedral particles morphology. After the pyrolysis at 800°C this particulate disappears in favor of honeycomb morphology (d). Observing this carbon to a higher magnification it can be noticed that is composed of open cell foam with very thin walls ((Fig 3 g). This indicates that during the carbonization the precursor is melted and is swollen by the volatile pyrolysis products. The pressure exerted by those volatiles was enough to break the bubbles prior to the solidification of the residue giving an interconnected porous network. The HD-NS looks similar to the -CD (Fig 3 b) except for the particles dimension (thinner for HD-NS sample) and after the pyrolysis the two carbons become even more similar, as observed at both low (Fig 3 e) and high

magnifications (Fig 3 h). The PY-NS particles appear similar to those of the previously described precursors (Fig 3 c), but surprisingly, after the pyrolysis, the carbon residue is composed of almost homogeneously distributed, spherical particles (Fig 3 f). This implies that the initial polygonal particles passed through a fluid phase before carbonization, during which the surface tension has prompted the spherical morphology. It is interesting to note that these particles are not stuck to each other but are physically distinct. These particles were broken by mortar grinding, observed at a higher magnification (Fig 3 i) and were found to be hollow. The morphology of the carbon obtained by PY-NS is thus totally different from those produced with the other precursors and the walls are thicker on average, indicating a greater amount of carbon. This result is interesting since carbon (hollow) spheres are functional carbon materials that have attracted much recent attention meanwhile they exhibit interesting structural and textural properties, because of their high specific surface area, low density, and high electrical and thermal conductivity [14,15].

In order to assess the carbonization pathway, TGA was performed. Fig. 4 shows the curves of weight loss and the rate of weight loss (DTGA) carried out in nitrogen flux to up 800°C of  $\beta$ -CD, PY-NS and HD-NS.

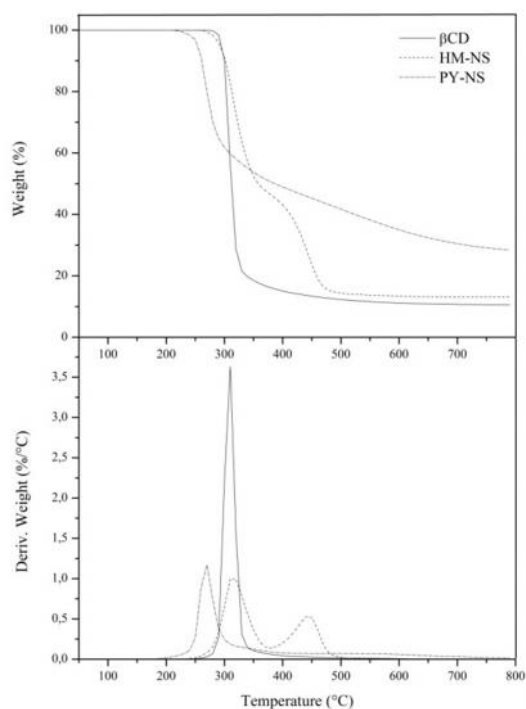


**Figure 4** TGA under nitrogen flow of  $\beta$ -CD and HD-NS, PY-NS nanosponges.

During the thermal degradation of -CD (solid line) a main step of weight loss followed by a char arrangement can be observed. The first step is very sharp and fast and occurs between 270°C and 400°C with a 90% weight loss. The second step starts from 400°C and is a slow thermal degradation of the char that proceeds till 800°C. The yield of carbon is about 9%.

The thermal degradation of PY-NS (dashed line) is also characterized by a pyrolysis followed by char arrangement behaviour, but the TGA profile is quite different. The first step occurs at lower temperature, between 220°C and 350°C, with a 42% of weight loss. The rate of weight loss is much lower than that of -CD, as observed comparing the DTGA curves. The second step goes from 350°C to 800°C showing a 14% of weight loss. The yield of carbon is three times higher than that observed for CD being about 28%.

In the thermal degradation curve of HD-NS (dotted line) two main steps of decomposition can be distinguished. The first one goes from 250°C to 350°C with 50% of weight loss while the second one from 350°C to 500°C with a 40% of weight loss. The char arrangements proceeds then till 800°C leaving 10% of carbon residue.

The chemical nature of the cross linker used to produce the NS strongly influenced the pyrolysis. The HDI seems to favour the reaction of volatilization that leads the NS to leave a small amount of char, whereas PYDA seems to improve the charring processes. Thus, in order to clarify the rule of the cross-linker in the thermal degradation behaviour, an ATR-IR analysis was carried out.

In Fig. 5, infrared spectra of solid residue from thermal degradation of nanosponges collected at several temperatures are reported: in the bottom half of the figure, sample spectra as such are reported and, moving up, the spectra obtained on TGA residues at increasing temperatures are observed.

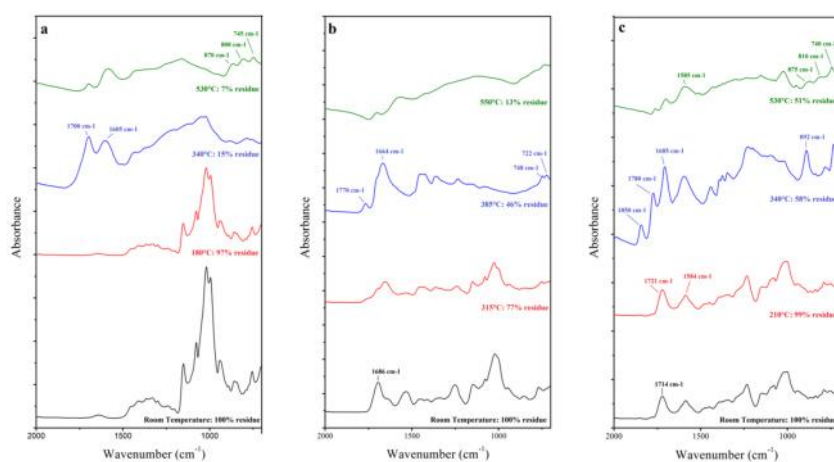


**Figure 5.** ATR Spectra of -CD (a), HD-NS (b) and PY-NS (c) at ambient temperature and after heating in TGA.

In general, all nanosponges show a similar trend at the rise of temperature that can be easily followed in the -CD trend. Firstly, samples show an intensity increase of the peak assigned to C=O bond stretching, found at about  $1700\text{ cm}^{-1}$  as heating proceeds, until it tends to disappear at high temperatures. Simultaneously, at about  $1600\text{ cm}^{-1}$ , signal assigned to stretching of C=C unsaturated species becomes stronger and stronger as temperature rises.

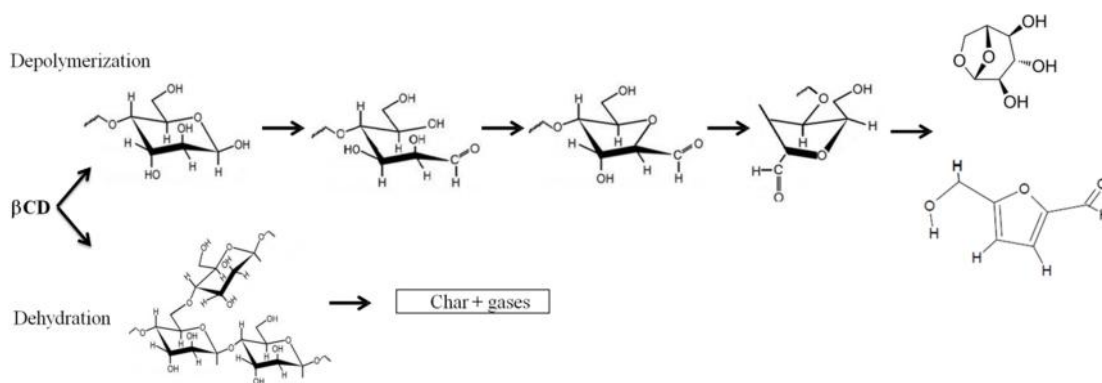
Signals in the range  $1200\text{-}900\text{ cm}^{-1}$ , attributable to C-O bond stretching of cyclodextrin portion of NS, tend to undergo a series of modifications at temperatures as high as  $350^\circ\text{C}$  disappearing at higher temperatures. In the portion of the spectrum between  $900$  and  $700\text{ cm}^{-1}$  the formation of aromatics species is evidenced by the appearance of the bands at  $865$ ,  $805$  and  $745\text{ cm}^{-1}$  ascribable to the out of plane deformation mode of aromatic C-H [16].

Moreover, each type of NS is characterized by distinctive signals, generated from the different nature of crosslinkers and crosslinking bridge-acting bonds. For instance, NS crosslinked by pyromellitic anhydride exhibits a gradual red-shift of  $1714\text{ cm}^{-1}$  signal confirming the transformation of ester bonds during pyrolysis (Fig. 5 C).

Otherwise, NS crosslinked by HDI exhibit signals assignable to urethane group (C=O stretching at  $1696\text{ cm}^{-1}$ , CHN stretching at  $1533\text{ cm}^{-1}$  and C-O-C stretching at  $1250\text{ cm}^{-1}$ ) Rising the temperature the urethane group decomposes and new bands indicate the formation of substituted urea at  $1664\text{ cm}^{-1}$  and isocyanurate at  $1770\text{ cm}^{-1}$  [17,18] (Figure 5 B).

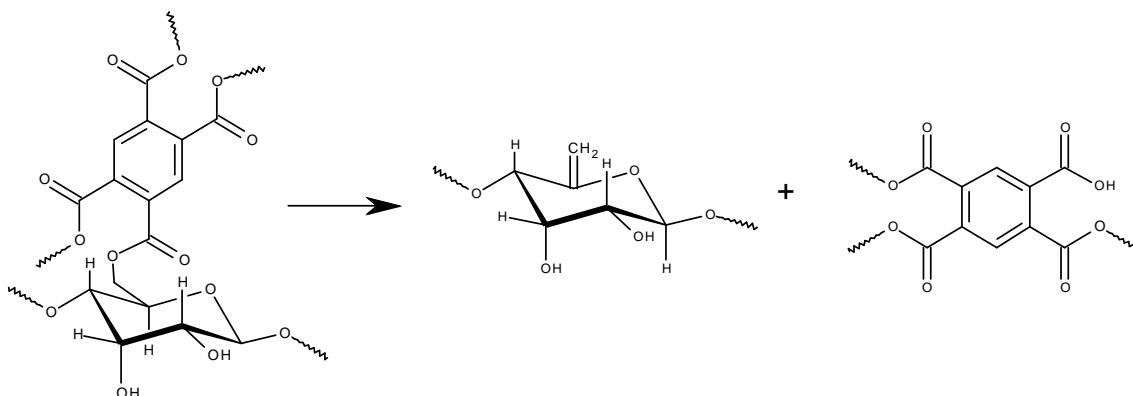
From these data, the conclusion is that pyrolysis advances by alteration of the saccharide structure and scission of bonds which constitute crosslinking bridges, resulting in the formation of desaturations which, becoming more and more numerous, act as precursors for reassembling of the structure, until the polycyclic aromatic structure typical of char.

In addition to crosslinkers effect, all the systems undergo a chemically similar charring process which is known for the plain -CD to be made of two competitive processes, the foster (depolymerization) following an intramolecular path and leading to the generation of volatile products, particularly levoglucosan; the latter (dehydration) following an intermolecular path that leads the system to the production of carbon residue and gas products such as  $\text{CO}_2$ ,  $\text{CO}$  and  $\text{H}_2\text{O}$  [10] (see Scheme 1).



**Scheme 1:** Mechanism of pyrolysis of the -CD [10].

It is therefore observed in the TGA experiments that the crosslinker substantially alters the amount of residue produced, affecting the competition between volatilization and carbonization in favor of the latter. NS exhibits crosslinking bridges based on bonds whose scission occurs easily and which leave behind cyclodextrin fragments which are able to interact together with an intermolecular mechanism resulting in the carbonization, reducing the effects of the intramolecular path which leads to volatilization. In detail, NS crosslinked by pyromellitic anhydride is characterized by the presence of an ester bridge which constitutes the thermally weaker bond of the whole system. It can pyrolyze allowing the extraction of a hydrogen atom from -CD (Scheme 2), giving rise to a carbon-carbon double bond which can promote the formation of the graphitic structure of char. The acidic species produced by ester pyrolysis may enhance the dehydration of the glucopyranose ring creating further carbon-carbon double bonds. Of course, a further contribution to the overall system carbonization can derive from the presence of aromatic groups in the structure, as reported in [19] (See scheme 2).



**Scheme 2** Mechanism of pyrolysis of PY-NS.

In the case of NS crosslinked by HDI, urethane bridges constitute the thermally weak bond of the system. Polyurethanes are normally subjected to two pyrolysis paths, whose kinetics are in competition: the former is a depolymerization path, which returns the starting material, (i.e. diisocyanate and polyol) causing high amounts of volatile products to form, while the latter is a dissociation path, which involves an hydrogen atom extraction, resulting in primary amines, CO<sub>2</sub> and olefins.

Electron donating group linked-urethanes are known to favor mainly the first process, resulting in the system tending to volatilization, while samples with an electron withdrawing portion target the second process, directing the system towards the production of unsaturated species, which are char polycyclic aromatic structure precursors. In view of the foregoing, higher carbonization efficiency could be shown by aromatic crosslinker that have an electron-withdrawing character like TDI.

#### 4. Conclusion

In this paper we describe our effort in producing a microporous carbon from hyper cross-linked CDs. The carbonization process was carried out with a simple heating ramp to 800°C on nanosponges prepared with two different crosslinking agents. Pyromellitic anhydride nanosponge (PY-NS) resulted effective to produce microporous carbon whereas nanosponge with HD (HD-NS) did not produce any porosity. The carbon from PY-NS shows a Langmuir specific surface area of 560 m<sup>2</sup>/g and a narrow pore size in the range of 5-16 Å corresponding to 0.08 cm<sup>3</sup>/g of total porosity. SEM observation reveals a peculiar morphology of the C-PY-CD carbon, composed of perfectly hollow spherical particles. The specific surface area of the carbon from the -CD is slightly lower than that of C-PY-CD with similar pore size. However, TGA shows that PY-NS is much more efficient precursor leading to a carbon yield that is 300% higher than -CD. The FT-IR studies show that this efficiency belongs to pyromellitic anhydride that influences the pyrolysis mechanism of -CD. This proceeds through a competition between the volatilization due to depolymerization of glucopyranose oligomers and charring due to intermolecular reaction. In the -CD clearly prevails the volatilization but the presence of PY favours the dehydrogenation, increasing the amount of carbon produced. HDI does not carry out this action and does not increase the amount of carbon with respect to the -CD.

In conclusion, the PY-NS has proved to be a good precursor for the production of carbon with a homogeneous and narrow distribution of micropores with a very simple carbonization process.

#### References

\* Corresponding Author, [marco.zanetti@unito.it](mailto:marco.zanetti@unito.it) (Marco Zanetti)

- [1] J. Rogers, A. Maznev, M. Banet, K. Nelson, *Adsorbents: Fundamentals and Applications*, 2000. doi:10.1146/annurev.matsci.30.1.117.
- [2] J. Lee, J. Kim, T. Hyeon, Recent progress in the synthesis of porous carbon materials, *Adv. Mater.* 18 (2006) 2073–2094. doi:10.1002/adma.200501576.
- [3] M.M. Bruno, G.A. Planes, M.C. Miras, C.A. Barbero, E.P. Tejera, J.L. Rodriguez, Synthetic Porous Carbon as Support of Platinum Nanoparticles for Fuel Cell Electrodes, *Mol. Cryst. Liq. Cryst.* 521 (2010) 229–236. doi:10.1080/15421401003720090.
- [4] L. Duan, Q. Ma, Z. Chen, The production of high surface area porous carbonaceous materials from polysiloxane, *New Carbon Mater.* 28 (2013) 235–240. doi:10.1016/S1872-5805(13)60078-5.
- [5] K.T. Cho, S.B. Lee, J.W. Lee, Facile Synthesis of Highly Electrocapacitive Nitrogen-Doped Graphitic Porous Carbons, *J. Phys. Chem. C.* 118 (2014) 9357–9367. doi:10.1021/jp501742x.
- [6] Y. Bao, G. Zhang, Study of adsorption characteristics of methylene blue onto activated carbon made by *salix psammophila*, in: *Energy Procedia*, 2011: pp. 1141–1146. doi:10.1016/j.egypro.2012.01.182.
- [7] H.C. Wang, B.L. Li, J.T. Li, P. Lin, X.B. Bian, J. Li, B. Zhang, Z.X. Wan, Direct synthesis of mesoporous carbon from the carbonization of hydroxypropyl- $\beta$ -cyclodextrin/silica composite and its catalytic performance, *Appl. Surf. Sci.* 257 (2011) 4325–4330. doi:10.1016/j.apsusc.2010.12.051.
- [8] S. V. Kurkov, T. Loftsson, Cyclodextrins, *Int. J. Pharm.* 453 (2013) 167–180. doi:10.1016/j.ijpharm.2012.06.055.
- [9] E.M.M. Del Valle, Cyclodextrins and their uses: A review, *Process Biochem.* 39 (2004) 1033–1046. doi:10.1016/S0032-9592(03)00258-9.
- [10] F. Trotta, M. Zanetti, G. Camino, Thermal degradation of cyclodextrins, *Polym. Degrad. Stab.* 69 (2000) 373–379. doi:10.1016/S0141-3910(00)00084-7.
- [11] B.H. Han, W. Zhou, A. Sayari, Direct preparation of nanoporous carbon by nanocasting, *J. Am. Chem. Soc.* 125 (2003) 3444–3445. doi:10.1021/ja029635j.
- [12] D. Wu, Y. Liang, X. Yang, Z. Li, C. Zou, X. Zeng, G. Lv, R. Fu, Direct fabrication of bimodal mesoporous carbon by nanocasting, *Microporous Mesoporous Mater.* 116 (2008) 91–94. doi:10.1016/j.micromeso.2008.03.018.
- [13] F. Trotta, M. Zanetti, R. Cavalli, Cyclodextrin-based nanosponges as drug carriers., *Beilstein J. Org. Chem.* 8 (2012) 2091–9. doi:10.3762/bjoc.8.235.
- [14] Q. Wu, W. Li, J. Tan, X. Nan, S. Liu, Hydrothermal synthesis of magnetic mesoporous carbon microspheres from carboxymethylcellulose and nickel acetate, *Appl. Surf. Sci.* 332 (2015) 354–361. doi:10.1016/j.apsusc.2015.01.195.
- [15] Q. Wu, W. Li, J. Tan, Y. Wu, S. Liu, Hydrothermal carbonization of carboxymethylcellulose: One-pot preparation of conductive carbon microspheres and water-soluble fluorescent carbon nanodots, *Chem. Eng. J.* 266 (2015) 112–120. doi:10.1016/j.cej.2014.12.089.
- [16] C. Morterra, M.J.D. Low, IR studies of carbons-II. The vacuum pyrolysis of cellulose, *Carbon N. Y.* 21 (1983) 283–288. doi:10.1016/0008-6223(83)90092-1.
- [17] M. Berta, C. Lindsay, G. Pans, G. Camino, Effect of chemical structure on combustion and thermal behaviour of polyurethane elastomer layered silicate nanocomposites, *Polym. Degrad. Stab.* 91 (2006) 1179–1191. doi:10.1016/j.polymdegradstab.2005.05.027.
- [18] S. Duquesne, M. Le Bras, S. Bourbigot, R. Delobel, G. Camino, B. Eling, C. Lindsay, T. Roels, Thermal degradation of polyurethane and polyurethane/expandable graphite coatings, *Polym. Degrad. Stab.* 74 (2001) 493–499. doi:10.1016/S0141-3910(01)00177-X.
- [19] Y. Sekiguchi, J.S. Frye, F. Shafizadeh, Structure and formation of cellulosic char, *J. Appl. Polym. Sci.* 28 (1983) 3513–3525. doi:10.1002/app.1983.070281116.

